

# **FILTERED SPHERICAL HARMONICS METHODS FOR TRANSPORT PROBLEMS**

**Ryan G. McClarren, Cory D. Hauck, and Robert B. Lowrie**

Computational Physics and Methods Group, Los Alamos National Laboratory

P.O. Box 1663, MS D413, Los Alamos, NM 87545, USA

ryanmc@lanl.gov      lowrie@lanl.gov

## **ABSTRACT**

We present a new way of using spherical harmonics expansions to solve transport problems. Our approach uses filtered expansions to give positive solutions and reduce wave effects in the solutions. We present two specific filters: one based on maintaining positivity in a  $P_1$  expansion, and the other that is a function of the total cross-section and the order of the expansion. We compare solutions using our filtered expansions to the standard spherical harmonics expansions, Monte Carlo, diffusion, discrete ordinates, and analytic transport solutions. These numerical results suggest that our filtered expansions give solutions that are comparable to other methods in terms of accuracy. Additionally, we point out how filtered spherical harmonics expansions could be improved.

*Key Words:* particle transport, spherical harmonics

## **1. INTRODUCTION**

Spherical harmonics expansions are one of the ways of treating the angular variable in the first-order form of the neutral particle transport equation [1, 2]. These expansions can be shown to be an asymptotic limit of the transport equation [3]. To get numerical solutions, the expansion must be truncated at some order, however, when scattering from the material medium is small, the truncated expansion can give nonphysical oscillations in the solution. These oscillations are the result of the spherical harmonics being the expansion that best approximates the transport solution in a least-squared sense [4]. These oscillations can cause the solution to become negative and make multiphysics simulations fail [5–7]. Moreover, it can be proven that for a given order of spherical harmonics expansion there exists a problem where the solution becomes negative [7].

The goal of this study is to eliminate the oscillations in the solution to the spherical harmonics ( $P_N$ ) equations and ensure that the solution is positive. We accomplish this by using filtered spherical harmonics expansions. These filters are based on finding the  $P_N$  expansion that minimizes the  $L^2$  norm of the error subject to a cost function related to the second angular derivative of the expansion. Such a filter is analogous to an artificial viscosity used in the numerical solution of hyperbolic conservation laws. Adding a cost function to the  $P_N$  expansion gives a general form for a filter with the strength of the filter remaining a free parameter. We give two prescriptions for choosing this filter strength. The first takes the  $P_1$  expansion and using the filter guarantees that this expansion is positive in the angular flux, in a similar manner to a slope limiter. The other filter chooses the filter strength based on the order of the expansion and the size of the total macroscopic cross-section of the material. As the order of expansion or the cross-section becomes larger, the filter strength decreases. Though we give two recipes for a filter, we do not assert that these are optimal. In fact, we suggest ways to create better filters.

In the following section we present the theory of filtered spherical harmonics expansions. For much of this section we follow the derivations given by Boyd [4]. We then concoct two filters and discuss their properties in Sec. 3. Section 4 discusses the  $P_N$  equations and how we solve them numerically. Numerical results are presented in Sec. 5, followed by a conclusions section.

## 2. FILTERED SPHERICAL HARMONICS EXPANSIONS

The spherical harmonics expansion takes the angular flux,  $\psi(\mathbf{x}, \hat{\Omega}, v, t)$ , and expands the angular variable  $\hat{\Omega} = (\mu, \varphi)$  in terms of spherical harmonics functions

$$\psi(\mathbf{x}, \hat{\Omega}, v, t) = \sum_{l=0}^{\infty} \sum_{m=-l}^l Y_l^m(\hat{\Omega}) \psi_l^m(\mathbf{x}, v, t). \quad (1)$$

where the spherical harmonics functions are given by

$$Y_l^m = (-1)^m \sqrt{\frac{2l+1}{4\pi} \frac{(l-m)!}{(l+m)!}} P_l^m(\mu) e^{im\varphi}, \quad (2)$$

$P_l^m(\mu)$  are the associated Legendre functions. The expansion coefficients in Eq. (1) are given by

$$\psi_l^m(\mathbf{x}, v, t) = \int_{4\pi} \bar{Y}_l^m(\hat{\Omega}) \psi(\mathbf{x}, \hat{\Omega}, v, t) d\hat{\Omega}. \quad (3)$$

The expansion in Eq. (1) must be made finite so that numerical computation can be performed. The most common means of making Eq. (1) finite is to truncate the series above a certain value of  $l = N$ ,

$$\psi_l^m = 0 \quad l > N. \quad (4)$$

Though this truncation is straightforward, it causes the solution to transport problems to have oscillations. Indeed, Boyd, when discussing truncated spherical harmonics expansions for general problems exclaims [4], “Truncating a [spherical harmonics] series is a rather stupid idea.” These oscillations can be explained by the fact that the spherical harmonics expansion is the minimizer of the functional

$$\mathcal{J} = \int_{4\pi} \left( \psi(\mathbf{x}, \hat{\Omega}, v, t) - \sum_{l=0}^{\infty} \sum_{m=-l}^l Y_l^m(\hat{\Omega}) \psi_l^m(\mathbf{x}, v, t) \right)^2 d\hat{\Omega}. \quad (5)$$

This functional can allow large oscillations about the true solution because it minimizes the square of the error.

Following Boyd [4], one can change the functional that is minimized to

$$\begin{aligned} \mathcal{J} = \int_{4\pi} \left( \psi(\mathbf{x}, \hat{\Omega}, v, t) - \sum_{l=0}^{\infty} \sum_{m=-l}^l Y_l^m(\hat{\Omega}) \tilde{\psi}_l^m(\mathbf{x}, v, t) \right)^2 d\hat{\Omega} \\ + \alpha \int_{4\pi} \left( \sum_{l=0}^{\infty} \sum_{m=-l}^l \nabla_{\hat{\Omega}}^{2k} Y_l^m(\hat{\Omega}) \tilde{\psi}_l^m(\mathbf{x}, v, t) \right)^2 d\hat{\Omega}. \end{aligned} \quad (6)$$

In this new functional  $\nabla_{\hat{\Omega}}$  is the gradient operator with respect to  $\hat{\Omega}$  and  $\alpha > 0$  is a parameter. This filter is, in a sense, adding artificial viscosity to the expansion: oscillations make this new term in the cost function large.

We will now find the new expansion coefficients,  $\tilde{\psi}_l^m$ . Noting that the spherical harmonics are eigenfunctions of the Laplacian operator on the sphere,

$$\nabla_{\hat{\Omega}}^2 Y_l^m = -l(l+1)Y_l^m, \quad (7)$$

one can show that

$$\tilde{\psi}_l^m = \frac{\psi_l^m}{1 + \alpha l^{2k}(l+1)^{2k}}. \quad (8)$$

Therefore, the filtered expansion forces the expansion coefficients to decrease with increasing  $l$ . These filters are also conservative in that they do not change the magnitude of  $\psi_0^0$  meaning that the scalar flux is unchanged. There still is the free parameter  $\alpha$  that we must specify. In this study we suggest two ways of defining  $\alpha$ , though we note that further research probably will uncover better filters.

### 3. TWO FILTERS

#### 3.1. Strictly Positive $P_1$ Reconstruction

The first filter that we describe is based on the  $P_1$  expansion of the angular flux. This expansion is

$$\psi = \frac{1}{2\sqrt{\pi}}\psi_0^0 + \frac{1}{2}\sqrt{\frac{3}{\pi}}\psi_1^0\mu + \sqrt{\frac{3}{2\pi}}\psi_1^1e^{-i\varphi}\sqrt{1-\mu^2}, \quad (9)$$

where we have used the relation that  $\psi_l^m = (-1)^m\psi_l^{-m}$  [8]. Notice that this reconstruction can be negative; when

$$|\psi_1^0| > \frac{\psi_0^0}{\sqrt{3}}, \quad (10)$$

or

$$|\psi_1^1| > \frac{\psi_0^0}{\sqrt{6}}, \quad (11)$$

then  $\psi$  will be less than zero for some combination of  $(\mu, \varphi)$ .

This possibility for a negative value suggests some kind of slope limiter. When  $\psi_1^m$  is too large we want to scale it back. The amount to scale it by is given in the modified reconstruction

$$\psi = \frac{1}{2\sqrt{\pi}}\psi_0^0 + \frac{1}{2}\theta_1\sqrt{\frac{3}{\pi}}\mu + \sqrt{\frac{3}{2\pi}}\theta_2\psi_1^1e^{-i\varphi}\sqrt{1-\mu^2}, \quad (12)$$

with

$$\theta_1 = \min\left(\frac{\psi_0^0}{\sqrt{3}|\psi_1^0|}, 1\right), \quad (13)$$

and

$$\theta_2 = \min\left(\frac{\psi_0^0}{\sqrt{6}|\psi_1^1|}, 1\right). \quad (14)$$

This reconstruction guarantees that  $\psi$  is positive.

We can cast the limited reconstruction of Eq. (12) as a filter by defining  $\alpha$  as

$$\alpha = \frac{1 - \theta}{2^{2k}}, \quad (15)$$

where the unadorned  $\theta$  is the minimum of  $\theta_1$  and  $\theta_2$ . With this definition of  $\alpha$  we then apply the filter as in Eq. (8).

One important property of this filter is that it only is applied where it is needed, i.e. in regions where the angular flux can be negative—when  $\theta = 1$  the filter does nothing. Also, in the diffusion limit it should not have an effect. This can be seen by the fact that in the diffusion limit  $\psi_1^m$  is an order  $\epsilon$  quantity whereas  $\psi_0^0$  is order one, so that  $\theta$  will be one.

There is a drawback to this filter in that it limits the  $P_N$  equations wavespeed to the  $P_1$  wavespeed,  $v/\sqrt{3}$  where  $v$  is the particle speed. This is a result of the hard limit we place on the size of  $\psi_1^m$ . For higher order  $P_N$  expansions, there are higher moments that can create a positive reconstruction with  $\psi_1^m$  outside the bounds of Eqs. (5) and (6). We believe that the reconstruction could be modified to ensure that the  $P_3$  expansion is positive. This would require devising conditions where a cubic is positive and we have not been successful to date in deriving such a condition. Even higher  $P_N$  expansions could be modified to give a positive reconstruction, though we believe as the order increases deriving positivity constraints becomes increasingly more difficult (and tedious). Finally, we point out that the slow wavespeed could be remedied by employing a  $P_{1/3}$  correction that adjusts the  $P_1$  wavespeed to be  $v$  [9].

### 3.2. Material Property Dependent Filter

The second filter we discuss does not explicitly guarantee a positive reconstruction of  $\psi$ , rather it imposes a filter in parts of the problem where the material interaction is weak. This filter writes  $\alpha$  as

$$\alpha = \frac{\omega}{(N^2 \sigma_t L + 1)^2}, \quad (16)$$

where  $N$  is the order of the  $P_N$  expansion,  $\sigma_t$  is the total macroscopic cross-section of the material,  $L$  is some characteristic length, and  $\omega$  is a positive number.

This filter has the property that as the order of the expansion increases, the filter affects the solution less. Therefore, as  $N \rightarrow \infty$  the solution does still converge to the transport solution. Moreover, this filter does not affect the diffusion limit: when  $\sigma_t$  is an  $O(1/\epsilon)$  quantity, then  $\alpha = 1 + O(\epsilon^2)$ . Perhaps the biggest upside to this filter is that it is linear in  $\psi_l^m$ . Unlike the filter based on the  $P_1$  reconstruction, this filter can be implemented in a straightforward manner.

At low expansion orders, for example  $P_1$ , this filter is strong in streaming regions. When  $\sigma_t = 0$  for  $N = 1$ ,

$$\tilde{\psi}_1^m = \frac{1}{1 + 4\omega} \psi_l^m, \quad (17)$$

regardless if the solution “needs” to be filtered or not. The other drawback to this filter is that it has a free parameter,  $\omega$ . Though this parameter gives flexibility to increase or decrease the filter strength, it would be better to have a prescribed value that guarantees positivity.

#### 4. THE SPHERICAL HARMONICS EQUATIONS

To show how we implement the filtered expansion, we begin with the equation for the time dependent transport of neutral particles,

$$\frac{1}{v} \frac{\partial \psi}{\partial t} + \hat{\Omega} \cdot \nabla \psi = S, \quad (18)$$

where  $\psi(\mathbf{x}, \hat{\Omega}, v, t)$  is the angular flux,  $v$  is the particle speed,  $\hat{\Omega}$  is the direction of flight variable,  $\sigma_t$  is the macroscopic interaction cross-section of the material, and  $S$  is a source function that takes into account the material-particle interaction, such as a scattering source. Also, we will be dealing with 2-D Cartesian geometry so that  $\nabla = (\frac{\partial}{\partial x}, \frac{\partial}{\partial z})$ . We then expand  $\hat{\Omega}$  in spherical harmonics functions as discussed above to get the system

$$\begin{aligned} \frac{1}{v} \frac{\partial \psi_l^m}{\partial t} + \frac{1}{2} \frac{\partial}{\partial x} (-C_{l-1}^{m-1} \psi_{l-1}^{m-1} + D_{l+1}^{m-1} \psi_{l+1}^{m-1} + E_{l-1}^{m+1} \psi_{l-1}^{m+1} - F_{l+1}^{m+1} \psi_{l+1}^{m+1}) \\ + \frac{\partial}{\partial z} (A_{l-1}^m \psi_{l-1}^m + B_{l+1}^m \psi_{l+1}^m) + \sigma_t \psi_l^m = S_l^m \quad \text{for } l = 1 \dots n, m = 1 \dots l \end{aligned} \quad (19a)$$

and

$$\frac{1}{v} \frac{\partial \psi_l^0}{\partial t} + \frac{\partial}{\partial x} (E_{l-1}^1 \psi_{l-1}^1 - F_{l+1}^1 \psi_{l+1}^1) + \frac{\partial}{\partial z} (A_{l-1}^0 \psi_{l-1}^0 + B_{l+1}^0 \psi_{l+1}^0) + \sigma_t \psi_l^0 = S_l^0 \quad \text{for } l = 0 \dots n, \quad (19b)$$

where

$$\begin{aligned} A_l^m &= \sqrt{\frac{(l-m+1)(l+m+1)}{(2l+3)(2l+1)}} & B_l^m &= \sqrt{\frac{(l-m)(l+m)}{(2l+1)(2l-1)}} \\ C_l^m &= \sqrt{\frac{(l+m+1)(l+m+2)}{(2l+3)(2l+1)}} & D_l^m &= \sqrt{\frac{(l-m)(l+m-1)}{(2l+1)(2l-1)}} \\ E_l^m &= \sqrt{\frac{(l-m+1)(l-m+2)}{(2l+3)(2l+1)}} & F_l^m &= \sqrt{\frac{(l+m)(l+m-1)}{(2l+1)(2l-1)}}. \end{aligned}$$

For the  $P_N$  method the scalar flux,  $\phi = \int_{4\pi} d\hat{\Omega} \psi$ , is given by  $\phi = 2\sqrt{\pi} \psi_0^0$ , and the number of unknowns in the  $P_N$  equations is  $\frac{1}{2}(n^2 + 3n) + 1$ . The initial conditions for  $P_N$  are given by

$$\psi_l^m(\mathbf{x}) = \int_{4\pi} d\hat{\Omega} Y_l^{m*}(\hat{\Omega}) \Psi(\mathbf{x}, \hat{\Omega}). \quad (20)$$

The boundary conditions we will use are ghost cell boundary conditions [5, 7] that are equivalent to the Mark boundary condition.

##### 4.1. Numerical Method

To solve Eqs. (19) we will use a linear discontinuous Galerkin method for the spatial discretization and a semi-implicit time integration method [10]. This approach has been shown to be robust in the diffusion limit, and it gives a straightforward means to apply our filters.

We apply the filters after each time step by computing  $\alpha$  in each spatial cell and then scaling  $\psi_l^m$  to get  $\tilde{\psi}_l^m$  as in Eq. (8). This approach is simple in that it allows us to treat any nonlinearity in the filter explicitly. How to deal with nonlinear filters with implicit solvers is an open question that we leave to future work, though we note that the filter given in Sec. 3.2 is linear and could be used with an implicit solver. We use  $\omega = 1/3$  for the material-based filter.

## 4.2. Sources

We present numerical results for two types of problems: linear problems with isotropic scattering and non-linear transport problems where the background material emits particles as a blackbody source.

### 4.2.1. Isotropic Scattering

For problems of linear transport with isotropic scattering and only one particle speed, the source function  $S$  becomes

$$S = \frac{\sigma_s}{4\pi} \phi - \sigma_t \psi, \quad (21)$$

where  $\sigma_s$  is the scattering macroscopic cross-section, and  $\sigma_t$  is the total macroscopic cross-section. This source makes

$$S_0^0 = -\sigma_a \psi_0^0, \quad (22)$$

$$S_l^m = -\sigma_t \psi_l^m, \quad l > 0. \quad (23)$$

### 4.2.2. Radiative Transfer Problems

In problems of the radiative transfer of grey x-rays [2] the source term is given by

$$S = -\sigma_a \left( \psi - \frac{acT^4}{4\pi} \right), \quad (24)$$

where  $a = 0.01372 \text{ GJ cm}^{-3} \text{ keV}^{-4}$  is the radiation constant,  $c = 2.998 \times 10^{10} \text{ cm/s}$  is the speed of light,  $\sigma_a$  is the absorption macroscopic cross-section, and the temperature  $T$  is governed by

$$C_v \frac{\partial T}{\partial t} = \sigma_a (\phi - acT^4). \quad (25)$$

The moments of  $S$  are then

$$S_0^0 = -\sigma_a \left( \psi_0^0 - \frac{acT^4}{2\sqrt{\pi}} \right), \quad (26)$$

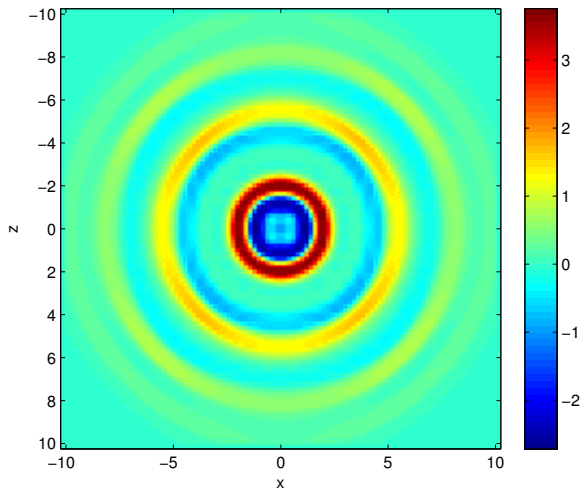
$$S_l^m = -\sigma_a \psi_l^m, \quad l > 0, \quad (27)$$

and Eq. (25) is, in terms of  $\psi_0^0$ ,

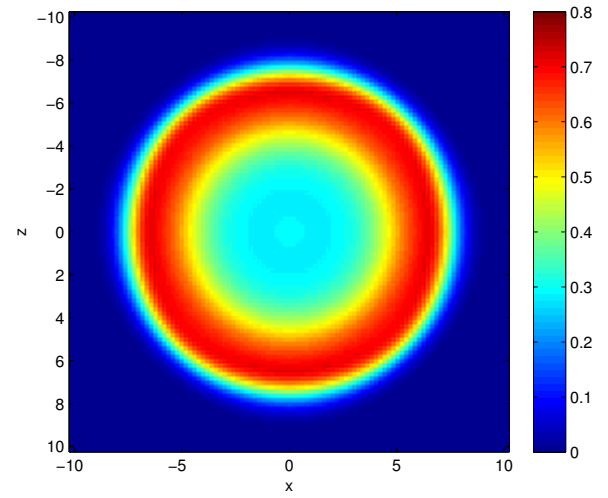
$$C_v \frac{\partial T}{\partial t} = \sigma_a (2\sqrt{\pi} \psi_0^0 - acT^4). \quad (28)$$

## 5. NUMERICAL RESULTS

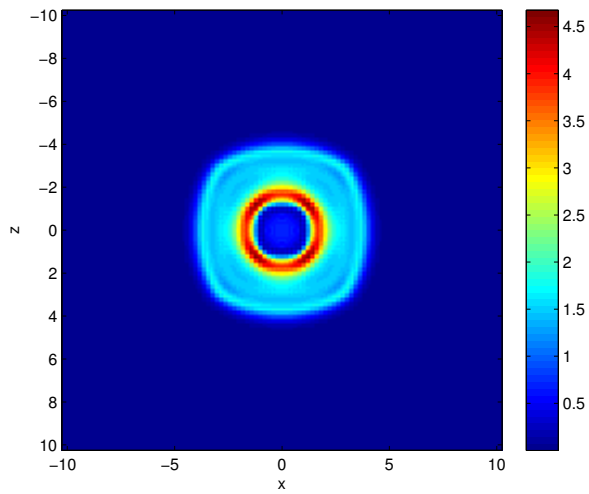
The first problem we solve is a linear transport problem as described in Sec. 4.2.1. This problem has an infinite line source pulsed at the origin at time 0. The material has  $\sigma_t = \sigma_s = 1$  and the particle speed is  $v = 1$ . There is an analytic transport solution to this problem given by Ganapol [11]. This is sort of a pathological problem due to the presence of a singularity in the solution at  $x/t = 1$ . Nevertheless, this



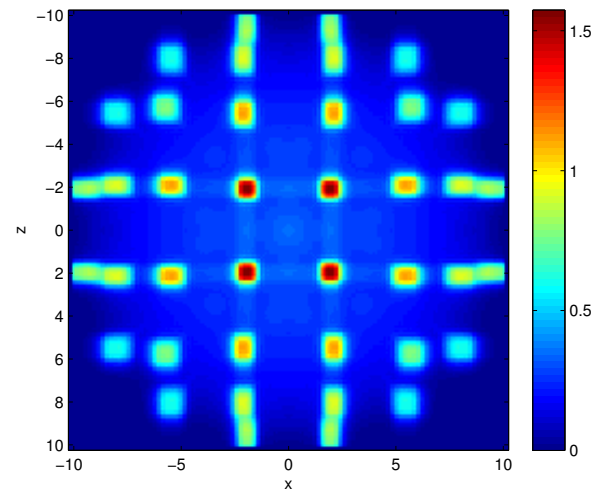
(a)  $P_7$



(b)  $P_7$  Material Filter



(c)  $P_7$  Slope Limited Filter



(d)  $S_8$

**Figure 1.** Solutions to the pulsed line source problem at  $t = 1$  using several methods.

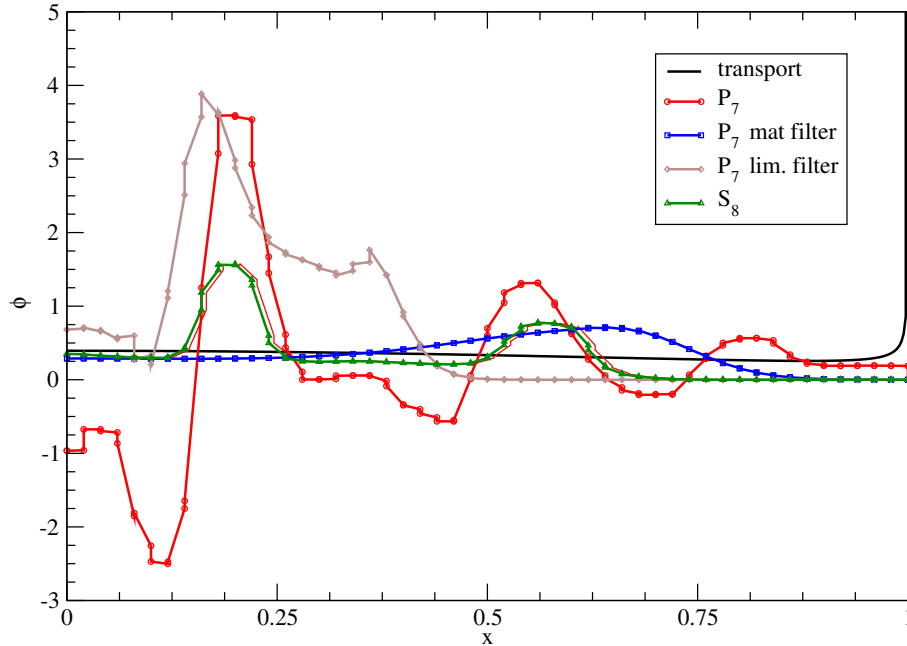


**Figure 2.** Comparison of solutions to the pulsed line source problem and  $t = 1$ .

solution shows that the standard  $P_N$  expansion can become negative (indeed the solution to the standard  $P_N$  equations for this problem has a *negative singularity*).

In Fig. 1, standard  $P_N$ , filtered  $P_N$ , and  $S_N$  solutions are compared on the line source problem at  $t = 1$ . Our numerical solutions used  $\Delta x = 0.01, 0.1$  for the  $t = 1$  and  $t = 10$  solutions respectively. The difficulty in solving this problem is apparent in the figure. The  $P_7$  solution has large amplitude waves that go negative, and the  $S_8$  solution has strong ray effects (though they look like “dot” effects on this problem). The two filtered spherical harmonics solutions both remain positive. The material-based filter does not have waves in the solution and is propagating information at nearly the correct speed. The slope-limiter filter moves information too slowly and does demonstrate wave-like behavior. These solutions are compared to Ganapol’s transport solution in Fig. 2. At this early time none of the numerical solutions adequately capture the transport solution. The solutions at a later time,  $t = 10$ , are shown in Fig. 3, where the  $P_7$  and  $S_8$  solutions give nearly the same results as the transport solution. The material-based filter and the slope-limiter filter are not as accurate. The slope-limiter filter has not moved information far enough into the problem, causing the solution near the origin to be too high. The material-based filter is also slightly too high near the origin. Despite these shortcomings of the filtered solutions we note that the solution at  $t = 10$  was arrived at without negativity or large wave (or ray) effects along the way.

The next problem that we solve is a radiative transfer problem first suggested in alternate form by Brunner [12]. This problem is a simplified hohlraum from an inertial confinement fusion experiment and is diagrammed in Fig. 4. A source of radiation is present on the left of the problem. This radiation flows into the problem and heats the block at the center.

The radiation field from this problem for different methods is shown in Fig. 5. The radiation is measured by the radiation temperature,  $T_{\text{rad}} = \sqrt[4]{\phi/a\bar{c}}$ . We compare the solution for our filtered spherical harmonics approximations to implicit Monte Carlo (IMC) [13], flux-limited diffusion, and  $S_8$  calculations. The implicit

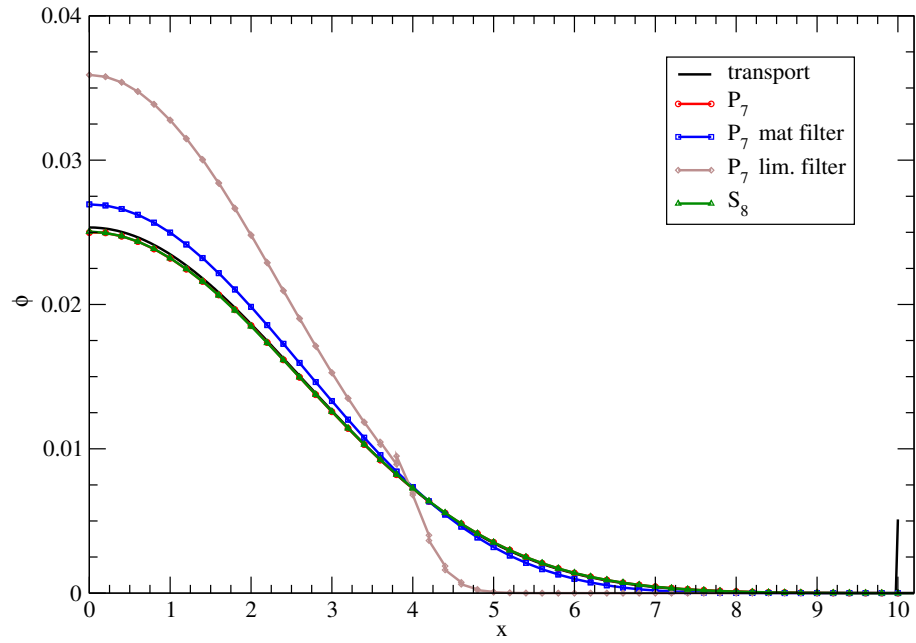


**Figure 3.** Comparison of solutions to the pulsed line source problem and  $t = 10$ .

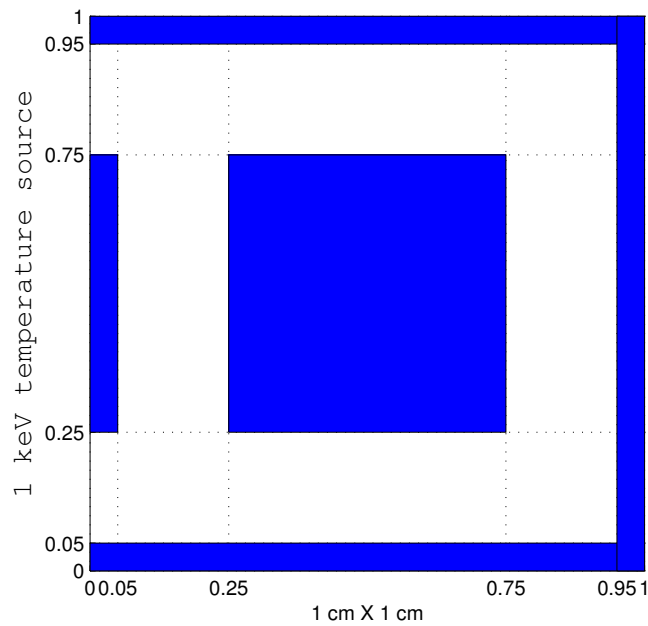


**Figure 4.** Layout for the 2-D hohlraum problem. The blue regions have  $\sigma_a = 100T^{-3} \text{ cm}^{-1}$  for  $T$  in keV. The white regions have  $\sigma_a = 0$ . Also,  $C_v = 0.3 \text{ GJ/cm}^3\text{-keV}$ .

Monte Carlo calculations used  $10^6$  particles per time step with a time step size of  $10^{-2}$  ns and 200 mesh cells per direction. The flux-limited diffusion solution used Larsen's flux limiter [14] with  $n = 2$  and 200 mesh cells in each direction. Our deterministic transport solutions,  $P_N$  and  $S_N$  used 100 cells per direction.

In Fig. 5 we compare several methods to solve the holhraum problem. For this problem the IMC solution is the most correct in terms of transporting radiation energy in a physically correct manner. Conversely, the flux-limited diffusion solution is the least correct because it allows radiation to flow around the block in the center of the problem. We do not show a  $P_7$  solution to this problem because the  $P_7$  radiation energy became negative and drove the material temperature negative causing the calculation to fail. The solution to the  $P_7$  equations with the slope-limiter filter appears to be similar to the IMC solution except that there is slightly more radiation to the right of the block than in the IMC solution. The  $P_7$  solution with the material-based filter has not moved the radiation far enough into the problem. This defect is mitigated by going to  $P_{11}$  with the material-based filter.

To better compare the methods we look at the radiation temperature along the line at  $y = 0.125$  cm in Fig. 6 and  $x = 0.85$  cm in Fig. 7. In Fig. 6 we see that the  $P_7$  solution with the slope-limiter filter is above the IMC solution with the  $S_8$  below the IMC solution. The material-based filter solutions dip below the IMC solution; the  $P_7$  version of this filter is far below the IMC solution near the right edge of the problem, and the  $P_{11}$  solution is closer to IMC but still below  $S_8$ . These comparisons hold on the right of the block as shown in Fig. 7 where the slope-limiter based filter solutions is higher than IMC, with the material-based filter solutions are below IMC.

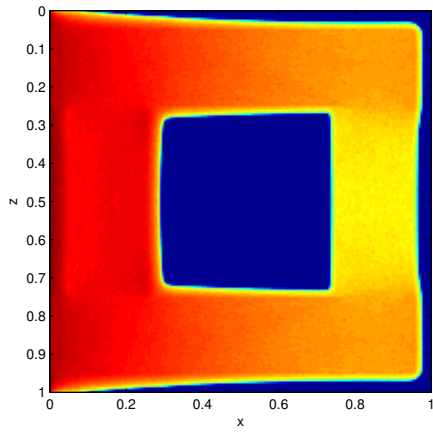
The material temperatures from different methods are compared in Fig. 8. In this figure we can see ray effects present in the  $S_8$  solution in the hot spots present on the right wall and the right side of the block. The  $P_7$  solution using the filter based on a linear reconstruction appears to be the closest to the IMC solution. The solutions using the material-based filter do not have enough heating on the right side of the problem compared to IMC.

## 6. CONCLUSION

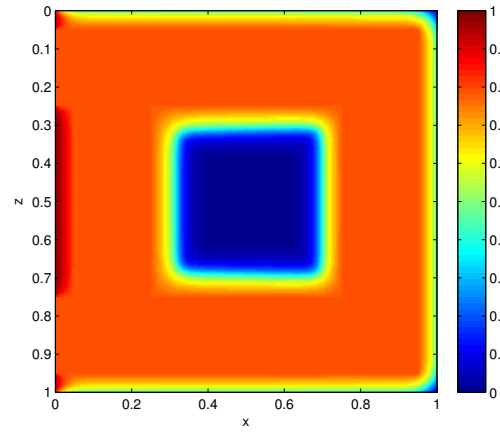
We have presented a general framework for developing filters for spherical harmonics approximations. We also developed two filters: one that guaranteed positivity using a limiter based on the  $P_1$  expansion, and one that enforced a decay in the expansion coefficients based on the material properties and the order of expansion. On the pulsed line source problem both filters gave positive solutions, however, both solutions also did not capture the transport solution at late times. On a multi-material problem of thermal radiative transfer the  $P_7$  solution using a filter based on a slope limiter applied to the  $P_1$  reconstruction was nearly as accurate as the  $S_8$ . This is significant because the filtered solution did not have negative energies or ray effects. On the same problem the material-based filter was not as accurate as  $S_8$  even when  $P_{11}$  was used.

We would like to again emphasize that the filters presented in this study are not likely the best filters for transport. Nevertheless, we believe that filters are a way to remove the drawbacks of the spherical harmonics equations. Possible directions for future work include a filter based on a positive  $P_3$  reconstruction, though this is certainly not the only way forward.

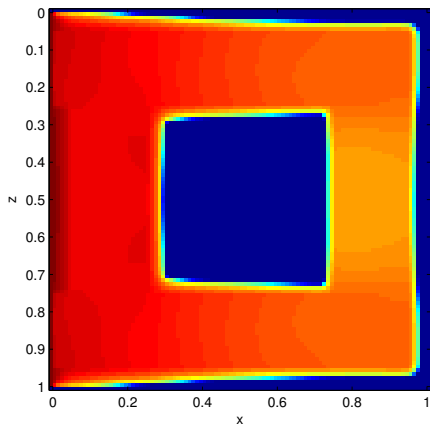
# Filtered Spherical Harmonics Expansions



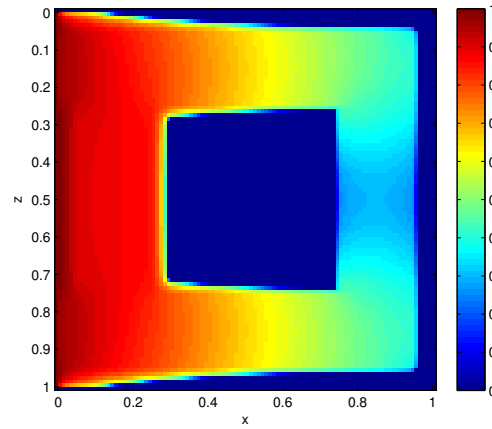
(a) Implicit Monte Carlo



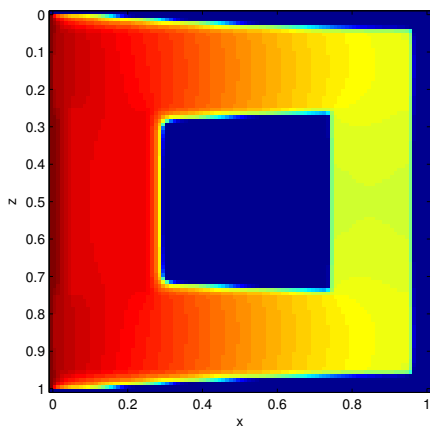
(b) Flux-limited Diffusion



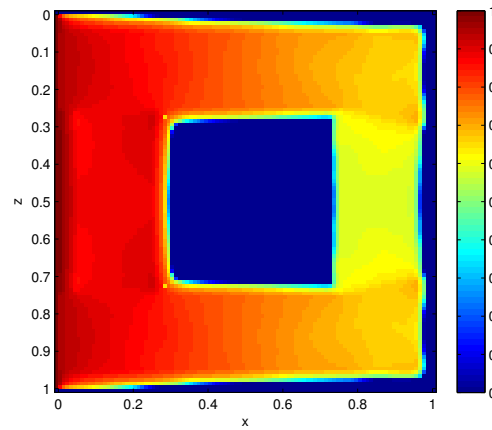
(c)  $P_7$  Slope Limited Filter



(d)  $P_7$  Material Filter



(e)  $P_{11}$  Material Filter



(f)  $S_8$

**Figure 5.** Radiation temperature solutions the hohlraum problem at  $t = 1$  ns.

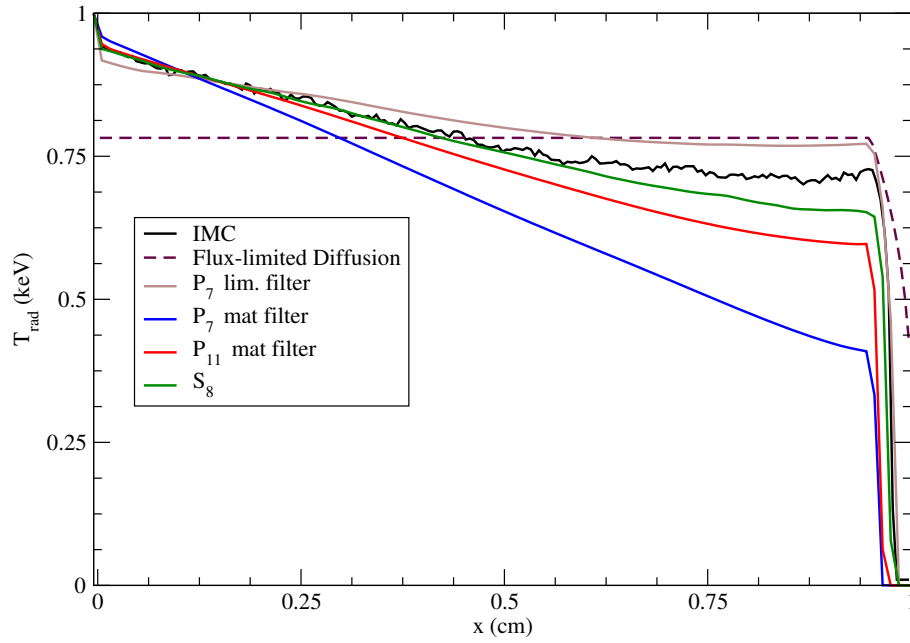


**Figure 6.** Radiation temperatures for the hohlraum problem at  $y = 0.125$  cm.

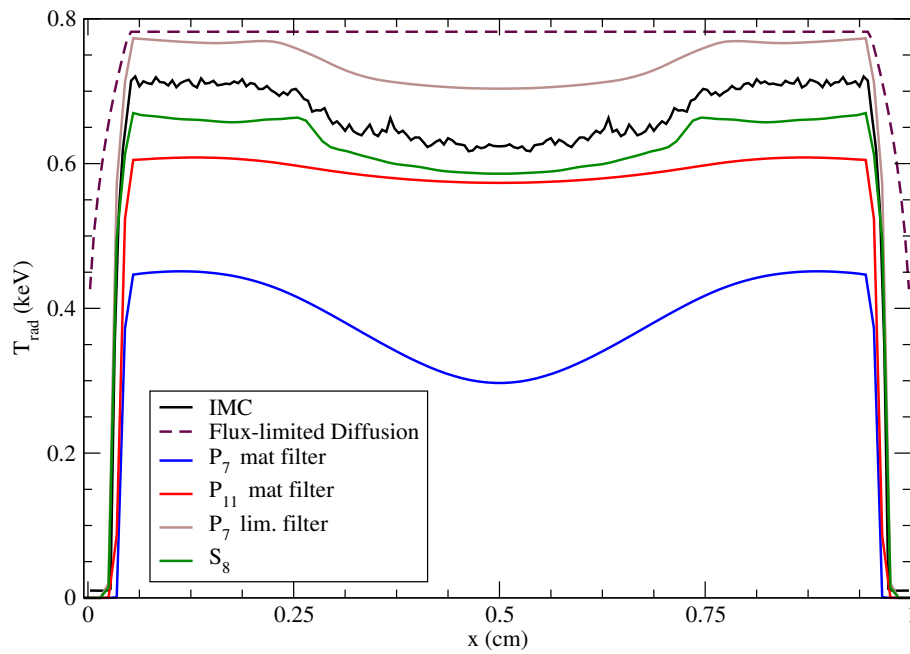
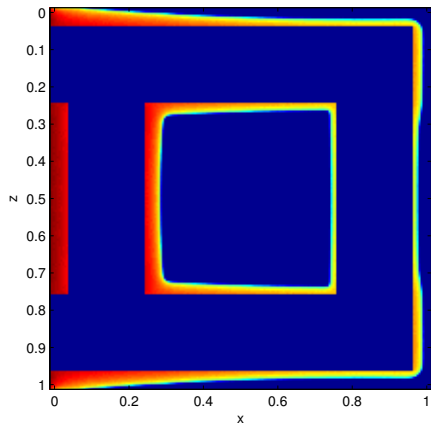
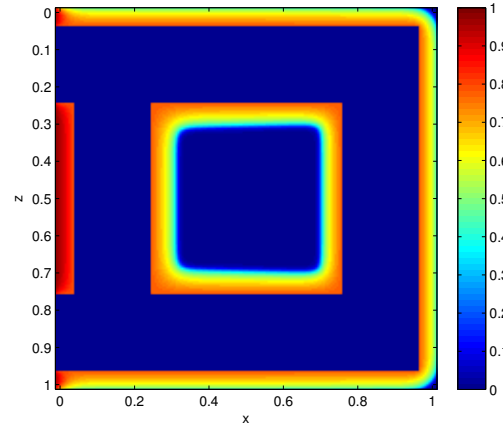


**Figure 7.** Radiation temperatures for the hohlraum problem at  $x = 0.85$  cm.

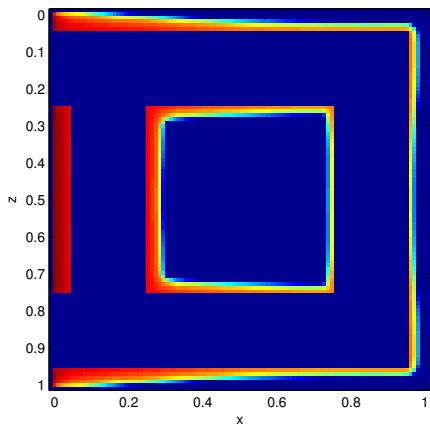
Filtered Spherical Harmonics Expansions



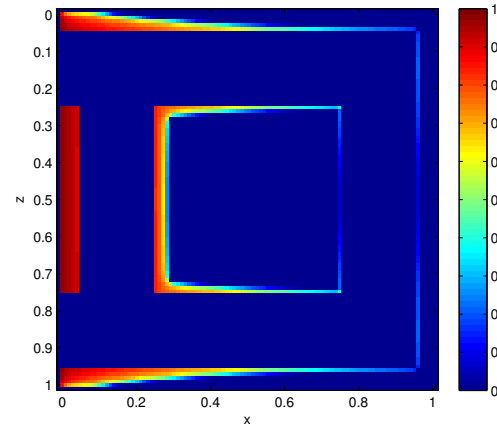
(a) Implicit Monte Carlo



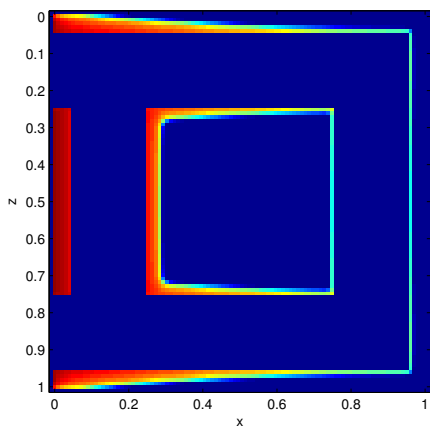
(b) Flux-limited Diffusion



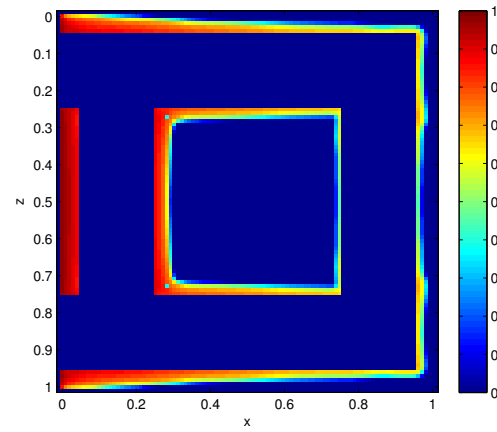
(c)  $P_7$  Slope Limited Filter



(d)  $P_7$  Material Filter



(e)  $P_{11}$  Material Filter



(f)  $S_8$

**Figure 8.** Material temperature solutions the hohlraum problem at  $t = 1$  ns.

## ACKNOWLEDGMENTS

This work was performed under U.S. government contract DE-AC52-06NA25396 for Los Alamos National Laboratory, which is operated by Los Alamos National Security, LLC. (LANS) for the U.S. Department of Energy. LA-UR-08-06446

## REFERENCES

- [1] G. I. BELL and S. GLASSTONE, *Nuclear Reactor Theory*. Malabar, Florida: Robert E. Kreiger Publishing, 1970.
- [2] G. C. POMRANING, *The Equations of Radiation Hydrodynamics*. Oxford: Pergamon Press, 1973.
- [3] E. W. LARSEN and G. C. POMRANING, “The  $P_N$  theory as an asymptotic limit of transport theory in planar geometry–I,” *Nucl. Sci. and Eng.*, vol. 109, no. 49, 1991.
- [4] J. P. BOYD, *Chebyshev and Fourier Spectral Methods*. Mineola, New York: Dover Publications, 2001.
- [5] T. A. BRUNNER and J. P. HOLLOWAY, “Two dimensional time dependent Riemann solvers for neutron transport,” *J. Comp. Phys.*, vol. 210, no. 1, pp. 386–399, 2005.
- [6] R. G. MCCLARREN, J. P. HOLLOWAY, and T. A. BRUNNER, “Analytic  $P_1$  solutions for time-dependent, thermal radiative transfer in several geometries,” *Journal of Quantitative Spectroscopy and Radiative Transfer*, vol. 109, pp. 389–403, Feb. 2008.
- [7] R. G. MCCLARREN, J. P. HOLLOWAY, and T. A. BRUNNER, “On solutions to the  $P_n$  equations for thermal radiative transfer,” *J. Comp. Phys.*, vol. 227, pp. 2864–2885, 2008.
- [8] T. A. BRUNNER, *Riemann Solvers for Time-Dependent Transport Based on the Maximum Entropy and Spherical Harmonics Closures*. PhD thesis, University of Michigan, Ann Arbor, Michigan, 2000.
- [9] G. L. OLSON, L. H. AUER, and M. L. HALL, “Diffusion,  $P_1$ , and other approximate forms of radiation transport,” *J. Quantitative Spectroscopy and Radiative Transfer*, vol. 64, pp. 619–634, 2000.
- [10] R. G. MCCLARREN, T. M. EVANS, R. B. LOWRIE, and J. D. DENSMORE, “Semi-implicit time integration for  $P_N$  thermal radiative transfer,” *J. Comp. Phys.*, vol. 227, pp. 7561–7586, 2008.
- [11] B. D. GANAPOL, “Homogeneous infinite media time-dependent analytic benchmarks for X-TM transport methods development,” tech. rep., Los Alamos National Laboratory, March 1999.
- [12] T. A. BRUNNER, “Forms of approximate radiation transport,” Tech. Rep. SAND2002-1778, Sandia National Laboratories, 2002.
- [13] J. A. FLECK, JR. and J. D. CUMMINGS, “An implicit Monte Carlo scheme for calculating time and frequency dependent nonlinear radiation transport,” *J. Comp. Phys.*, vol. 8, pp. 313–342, 1971.
- [14] J. MOREL, “Diffusion-limit asymptotics of the transport equation, the  $p_{1/3}$  equations, and two flux-limited diffusion theories,” *J. Quantitative Spectroscopy and Radiative Transfer*, vol. 65, pp. 769–778, 2000.